

Scientific report

regarding the project implementation between January - December 2013

1.3. Numerical modeling of fluid flows for different values of the magnetic field and electric current for an isothermal configuration with 4 electrodes

The closing of the electric circuit can be also achieved with four electrodes symmetrically placed on the free surface level, as it is shown in fig. 1. The electrodes are placed along the diagonals, at equal distances from the center of the free surface. The electric current is introduced in the circuit using two power supplies. The electrode connection to the power supplies is done in such way that on each diagonal we have a anode and a cathode.

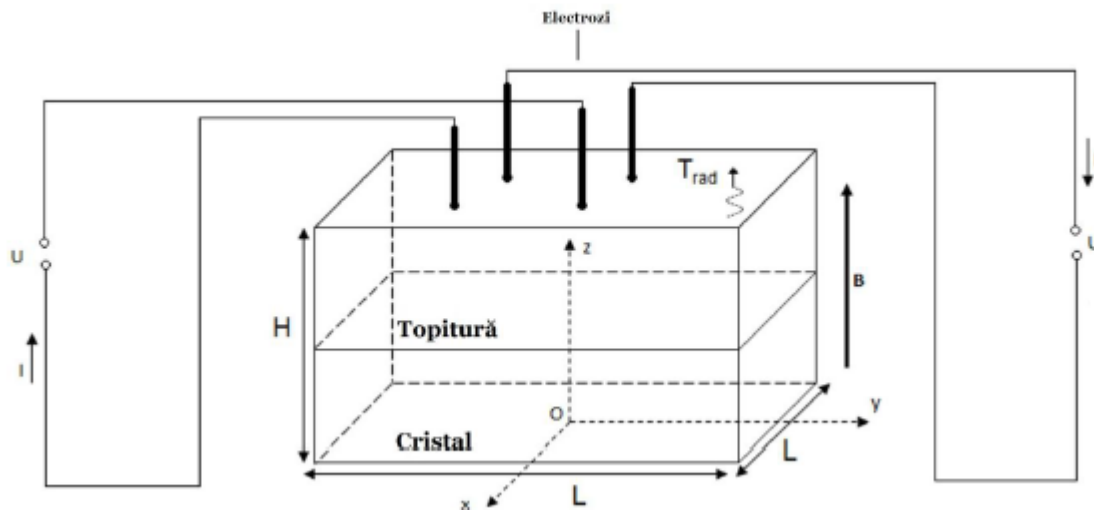


Figure 1. The four electrodes numerical model schematic used for the numerical modeling of the growth process of multicrystalline Si using the directional solidification method

Similar to the two electrode configuration, the modeling experiments done in these conditions used the 2 A, 5 A, 10 A values for the electric current intensity and 10 mT for the magnetic field induction. The melt behavior in these three situations is similar to the case of two symmetrically placed electrodes (fig. 2). At $I = 2$ A, we can notice the presence of four vortices, each centered in the contact point of the electrodes with the melt. As the current intensity increases, the symmetry is broken, leading to the formation of one single vortex. The rotation velocities are significantly lower than for the other configurations, with one or two electrodes, thus needing a much longer time interval for the homogenization of the melt. These continue to depend on the applied electric current intensity values. Thus, for $I = 2$ A the rotation velocity in the melt reaches the value of 7.6 rpm, increasing to 10.7 rpm for $I = 5$ A and at 12 rpm for $I = 10$ A.

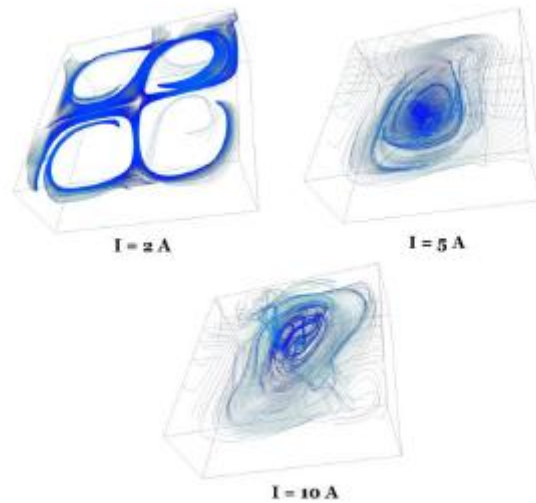


Figure 2. The melt flow orientation near the solidification interface for the four electrodes configuration, at different intensities of the electric field (2, 5, 10 A). $B = 10 \text{ mT}$

At low intensities of the electric current ($I = 2 \text{ A}$), the central area of the melt is weakly affected by the rotational velocities around the electrodes. Except the $I = 2 \text{ A}$ case, the thermal field and the flow velocity at the free surface of the melt level are asymmetric and unpredictable (Fig. 3). Considering these, it is notable that at high values of the intensity, $I = 5 \text{ A}$; 10 A , the velocity in the center of the melt rises, preventing the precipitates accumulation.

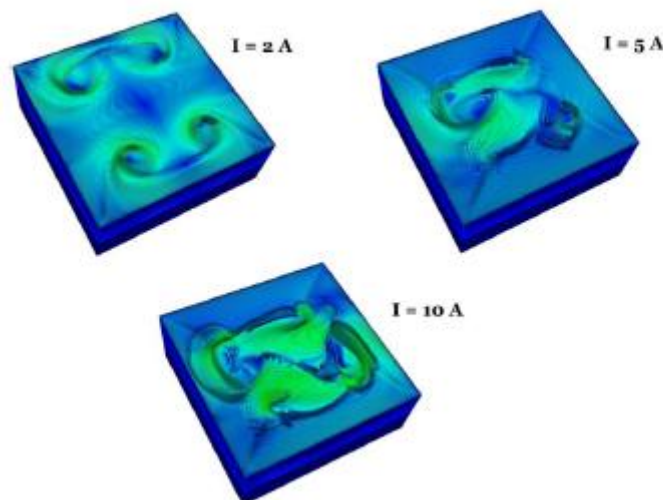


Figure 3. The flow velocities representation at the melt free surface

In fig. 4 the solidification interface shapes are shown for the 2 A , 5 A and 10 A cases, in correlation with the interface computed for the natural convection case. The interface deflection is lower than the natural convection case, its height not surpassing 0.2 cm . Unlike the other configurations with one or two electrodes, in this case, the interface deflection doesn't grow proportionally with the applied electric current. For $I = 2 \text{ A}$, the maximum deflection reaches 2 maxima in the area where the

electrodes touch the melt, equilibrium which is broken at 5 A and 10 A. So, we can state that applying an electromagnetic field using the four electrodes configuration doesn't offer a precise control over the solidification interface.

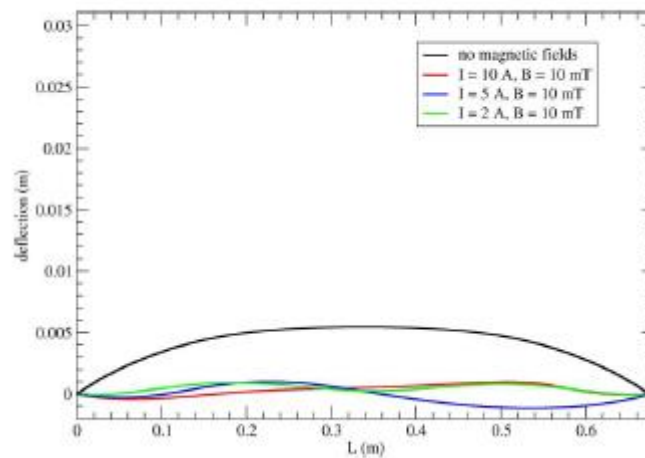


Figure 4. Solidification interface shape for the convection under the influence of a electromagnetic field composed of a stationary magnetic field of $B = 10$ mT induction and a direct electric current at different values of the intensity, applied with the help of four electrodes

1.4. Development of STHAMAS3D software for usage on IBM BlueGene supercomputer

To obtain a real solution starting from an arbitrary one using STHAMAS3D, at least 800 seconds are needed in real time, with a time step of 0.1 seconds. This implies a high computational effort for the parametrical studies. From that reason, the simulation software STHAMAS3D was modified in order to be used on one of the most powerful supercomputers, the BlueGene/P, made available by the West University of Timisoara for the execution of high performance computations.

The UVT BlueGene/P supercomputer has the following characteristics:

- computing power
 - 1 x BG/P Rack
 - CPU: 1024x Quad PowerPC 450 @850Mhz
 - RAM: 4GB/CPU
 - inter-connect: 3D-Torus network
- storage system
 - 2x I/O Nodes
 - 2x IBM DS3524 SAN's
 - HDD: 48x 320GB SAS
 - connectivity: 10GbE Ethernet

The results obtained after running the simulation on BlueGene/P were compared with the ones obtained after running the same input on the Nanosim cluster of the Faculty of Physics in the frame of West University of Timisoara. Nanosim is a HP-AMD-Opteron 2.2 GHz (1 Gbit/s switched) cluster with 12 compute nodes.

The geometry used is formed from melt and silicon crystals with the $38 \times 38 \times 40 \text{ cm}^3$ dimensions. The time-dependent tridimensional computations have been done with the STHAMAS3D software, whose libraries and subroutines were adapted to run both on the Nanosim cluster and on the BlueGene/P supercomputer.

The computational domain is subdivided in two blocks, one corresponding to the melt area and one corresponding to the crystal area. For each block we have 50 nodes on the x and y directions and 70 nodes on the z direction, corresponding to a computation grid of 350000 control volumes.

STHAMAS3D requires several iterations on each time step for solving time-dependant equations. In the parameters input files, the maximum number of iterations done at each time step can be set. If the convergence criteria is achieved before doing the maximum number of iterations, the software moves to the next time step. For the test done, the run time was measured after 1000 iterations and 10 respectively 25 intermediate steps were considered.

The results obtained for the run time on the two computation systems are presented in fig. 1.

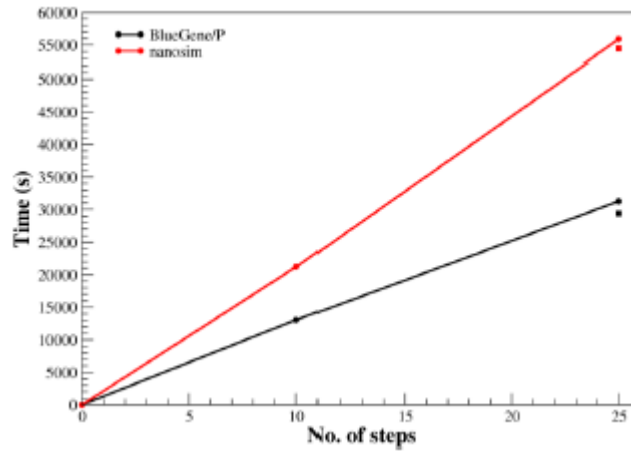


Figure 1. The run time of STHAMAS3D on different computation systems in different conditions

We can observe from Figure 1 that at each time step 10 intermediary iterations are done, the run time on Nanosim is 21207.672 s, and 13048.5 s on BlueGene/P. This means that by adapting the code to run on the BlueGene/P supercomputer we obtained an almost 40% reduction of the total run time.

If each time step there are 25 intermediary steps done, like expected, the total run time increases, but also the difference noted between the run time on BlueGene/P and Nanosim increases. In this case, after 1000 iterations, the total run time registered on BlueGene/P is 44% smaller than the run time registered on Nanosim, under the same parameters for the STHAMAS3D simulation software.

In the cases presented above, the simulation results are written at every 100 iterations. It is a known fact that the process of writing the data in the output files might be computationally expensive, and so we have studied a case where the results are written once, at the end of the 1000 iterations. The registered values are marked with squares in Fig. 1. It can be noted that, both on BlueGene and also on Nanosim, the run time, after 1000 iterations is lower than the case where the output is written also at intermediary time steps. This decrease isn't significant and such the proportion between the run time registered on the two systems is the same as the previous cases.

2.4. Measurements of fluid flow velocity for different values of the magnetic field and electrical current

With the ultrasound velocimeter DOP3010 bought and commissioned in activity 2.3 fluid flow velocity measurements were made for the experimental set-up obtained in activity 2.2. Thus, in a plexiglass crucible that emulates the shape of industrial crucibles used for obtaining directional solidified multicrystalline silicon a mixture of GaInSn liquid at room temperature was poured. This alloy is put in contact with an electrical current through two electrodes placed in the crucible lid. Two configuration for the electrodes have been chosen: a symmetrical one, with the electrodes placed at one third and two thirds of the diagonal length respectively, and an asymmetrical configuration with one electrode placed in the center of the crucible and the other one place at one third from the crucible corner. These two configurations are shown in Figure I.

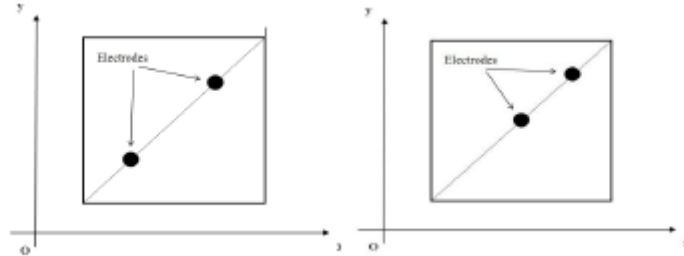


Figure I. a) Symmetrical configuration; b) asymmetrical configuration of the electrodes

The crucible was placed in the air gap of the C shaped electromagnet (made in activity 2.1) as can be seen in Figure II. A vertical magnetic field of 10 mT (for both configurations) and 3 mT (only for the symmetrical configuration) was applied.

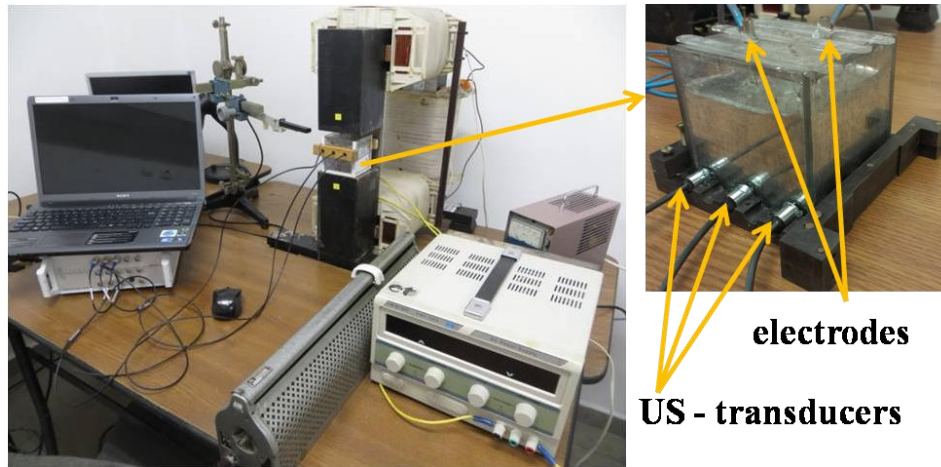


Figure II. Experimental configuration with electromagnet, velocimeter with ultrasonic transducers, crucible filled with GaInSn melt put in electrical contact with electrodes connected to a DC power supply

Perpendicular to the crucible an assembly with ultrasonic sensors (transducers) was fitted at three levels of height (5 mm, 25 mm and 40 mm) thus depth velocity profiles (the velocity axis projection passes through the center of each transducer) are measured at the same time for three positions (9 mm, 35 mm and 61 mm). These measurements were done for the chosen magnetic field values for the two electrodes configurations using 2 A, 5 A and 10 A for the electrical current.

Asymmetrical configuration

For all the measurements, independent of the shape of the profile corresponding to a fluid flow, it can be seen that as the value of the electrical current intensity increases the flow (profile) stays the same but with increasing values of the velocity.

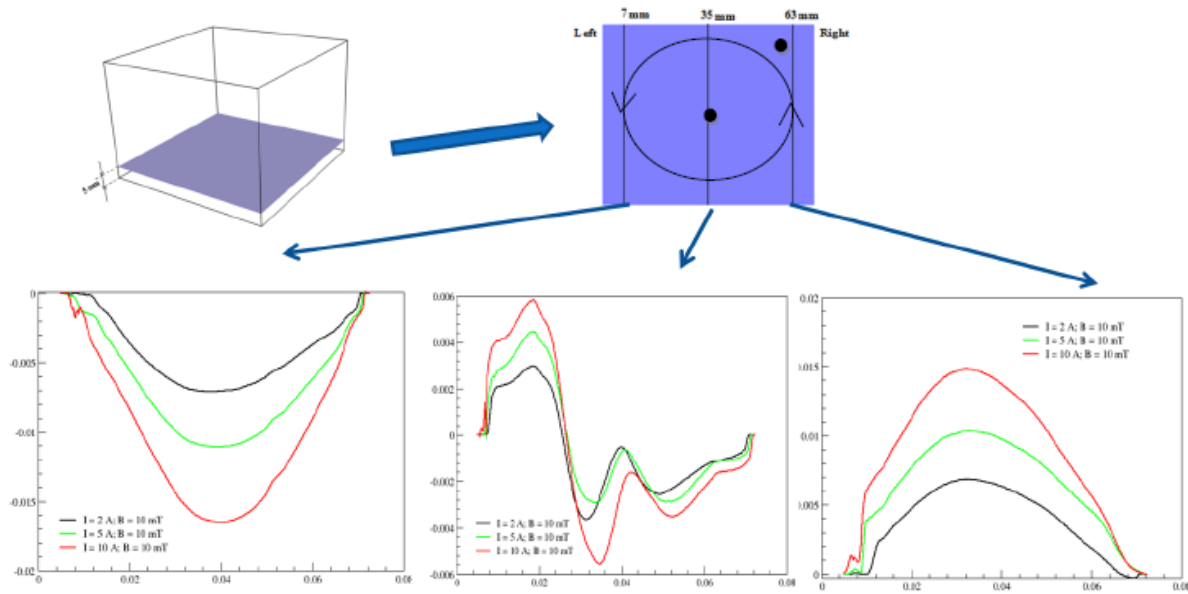


Figure III. Velocity profile along the axis of the three transducers placed at 9 mm, 35 mm and 61 mm from the left crucible wall in the plane situated at 5 mm from the crucible bottom for $I = 2$ A, 5 A and 10 A at $B = 10$ mT, for an asymmetrical electrodes positioning

Figure III shows the velocity profiles along the axis of the three transducers at 5 mm. The fluid flow seems to be completely dominated by the electrode placed in the middle. The velocity profiles at 9 mm and at 61 mm have a negative value with a maximum in the middle and a positive value with a maximum position in the same way, thus indicating a rotational movement around the center. The velocity profile at 35 mm indicates a transition from the fluid flow towards the sensors in the first half and from the sensor in the second half, the central maximum being explained by the existence of a central vortex structure prolonged downwards on the electrode's axis. Besides, the highest velocity values of all the asymmetrical profiles is registered here, this being consistent with the contact between the vortical structure and the crucible bottom that can lead to a flow recirculation in the horizontal plane of the flow component that goes downwards through the vortex.

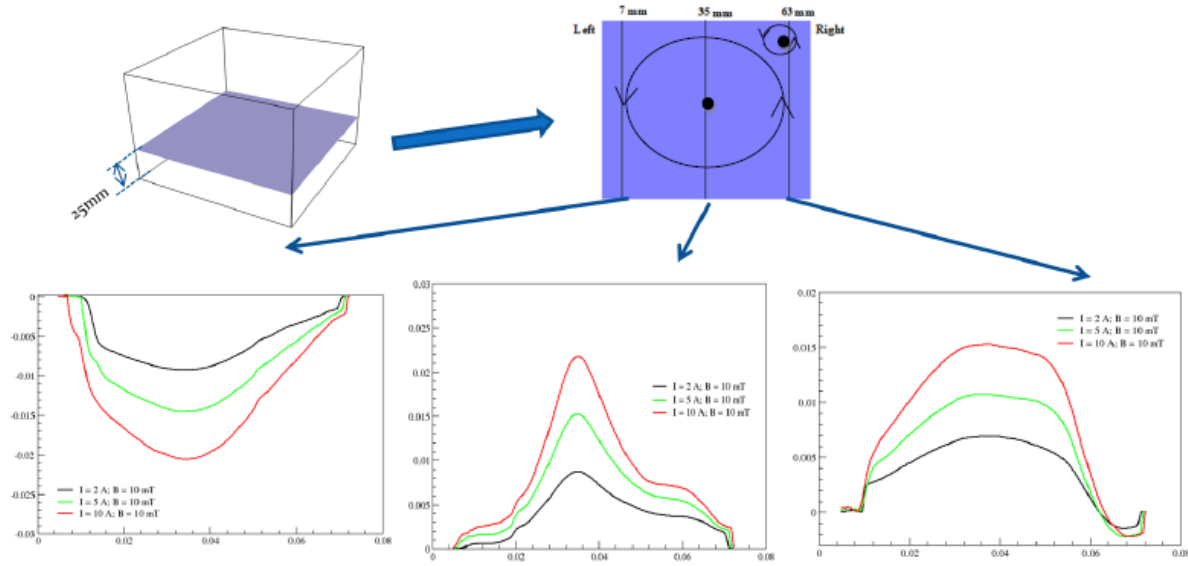


Figure IV. Velocity profile along the axis of the three transducers placed at 9 mm, 35 mm and 61 mm from the left crucible wall in the plane situated at 25 mm from the crucible bottom for $I = 2$ A, 5 A and 10 A at $B = 10$ mT, for an asymmetrical electrodes positioning

In Figure IV, that represent the velocity profiles corresponding to the plane situated at 25 mm from the bottom, shows the same behavior of the central electrode that dominates the flow structure. The middle profiles doesn't indicate a change of the flow direction, it only shows a central maximum of the rotation velocity that can be an indication of the lateral displacement of the rotation center. A closer look at the velocity profile from the right hand side (61 mm) also shows at the end the effect of the electrode asymmetrically placed that determines a rotation in the opposite direction thus explaining the negative values at the end of the profile.

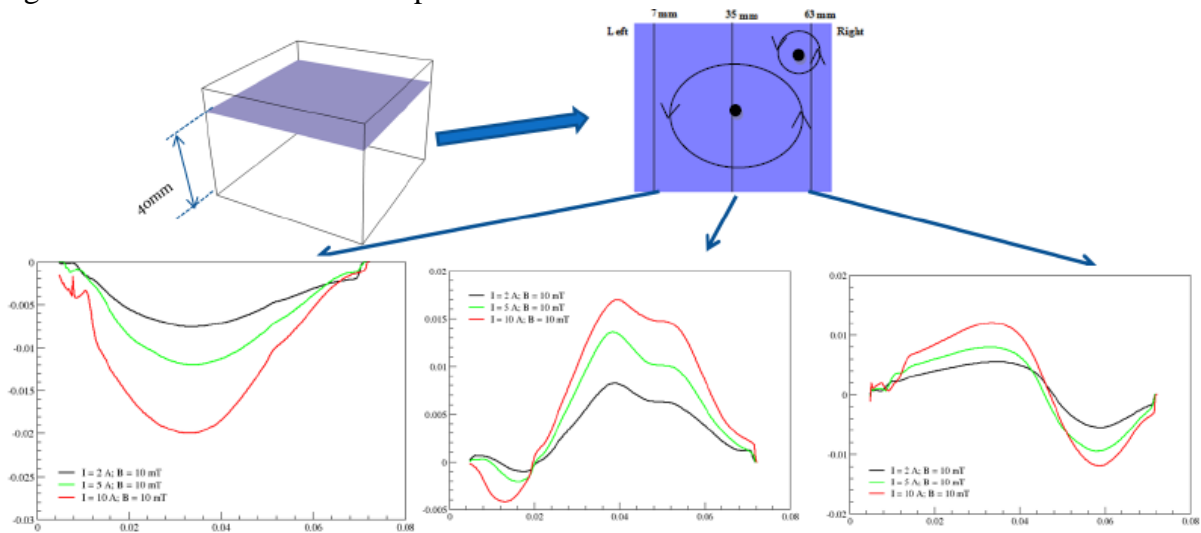


Figure V. Velocity profile along the axis of the three transducers placed at 9 mm, 35 mm and 61 mm from the left crucible wall in the plane situated at 40 mm from the crucible bottom for $I = 2$ A, 5 A and 10 A at $B = 10$ mT, for an asymmetrical electrodes positioning

Figure V shows the velocity profiles corresponding to the 40 mm plane. The situation seems to be similar to the one presented in Figure IV indicating a displacement of the central vortex towards left and a higher influence of the lateral electrode (the change of the flow direction at the end of the 61 mm profile). For the 35 mm profile the maximum velocity is smaller (0.015 m/s compared to 0.02 m/s at 25 mm) but they are distributed over a longer length this being consistent with the fact that probably more melt from the free surface is directed towards the bottom similar to a liquid that flows through a funnel. (vertical vortex).

Symmetrical configuration

For all the measurements, independent of the shape of the profile corresponding to a fluid flow, it can be seen that as the value of the electrical current intensity increases the flow (profile) stays the same but with increasing values of the velocity. This behavior changes if a smaller magnetic field is applied (3 mT and an electrical current of 10 A). The change of the electrical current intensity has an influence on the flow source term (the Lorentz force that is the product between the current density with the magnetic field), while the change in the magnetic field, besides modifying the Lorentz force, has also an effect related to the dampening of the vertical flow recirculation (the direction on the magnetic field), flow that is different for different values of the magnetic field [1].

In order to understand the flow structure for the symmetrical configuration of the electrodes, that is more complex than in the case of the asymmetrical configuration, a first analysis closer to the surface is required. In Figure VI the velocity profiles at 40 mm from the bottom are represented. The profile at 9 mm indicates a stronger flow in the direction from the sensor (positive), closer to the electrode and a weaker flow in the opposite direction, further from the origin. The 61 mm profile indicates a weaker flow towards the sensor (negative values of the velocity) closer to the origin and a strong positive flow, around the electrode. This can be explained by the existence of two convection loops around the electrodes that move in opposite directions, behavior also confirmed by the visual observations done at the melt surface. The 35 mm velocity profile gives a confirmation of the flow towards the sensor originating from both the electrodes, but also gives an indication of the fact that the maximum flow velocity is moving outside the median line towards the secondary diagonal (the one that doesn't contain the electrodes). Visual observations on a similar configuration with an aqueous solution of NaOH indicated the possibility of a flow towards the bottom corner of the smaller crucible diagonal (in Figure VI) that touches the walls and then is recirculated downwards in the vertical plane.

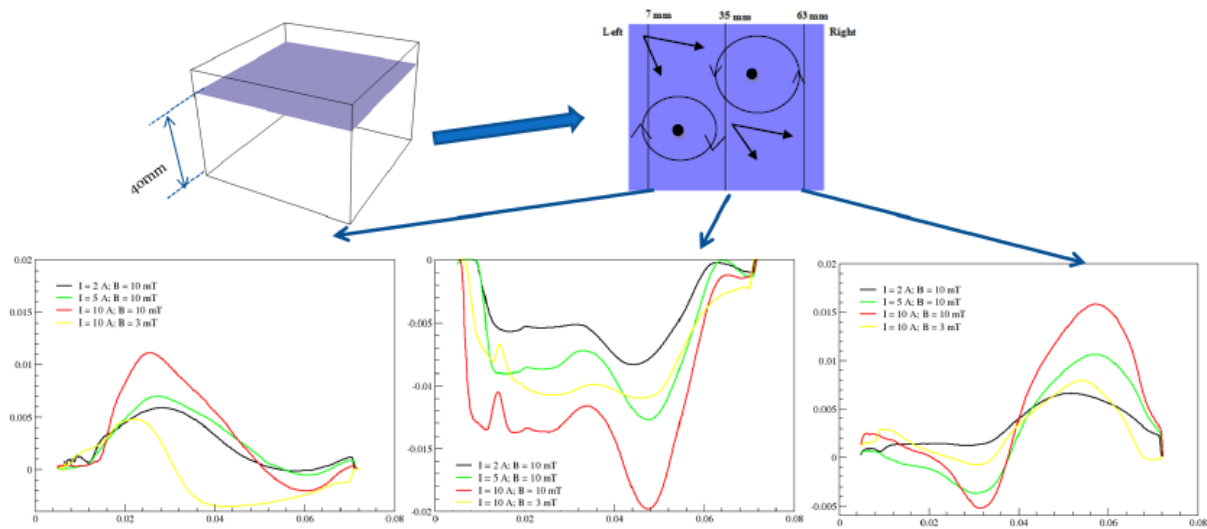


Figure VI. Velocity profile along the axis of the three transducers placed at 9 mm, 35 mm and 61 mm from the left crucible wall in the plane situated at 40 mm from the crucible bottom for $I = 2 \text{ A}$, 5 A and 10 A at $B = 3 \text{ mT}$, for a symmetrical electrodes positioning

In Figure VII the velocity profiles for the fluid flow at 25 mm from the bottom are represented. The characteristics of the fluid flow at 40 mm are kept here as well but the structure seems to be more complex, possibly turbulent.

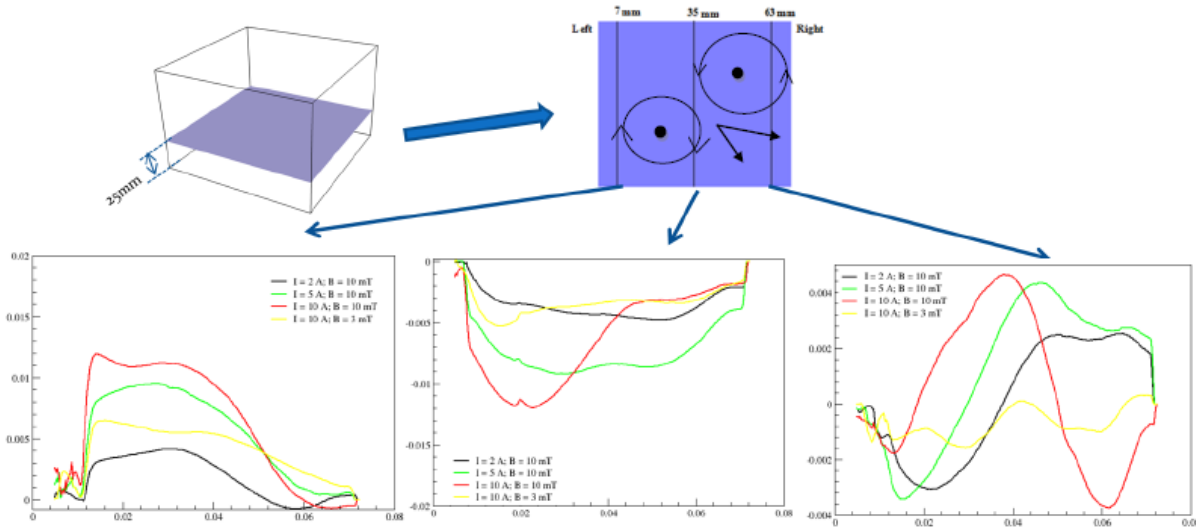


Figure VII. Velocity profile along the axis of the three transducers placed at 9 mm, 35 mm and 61 mm from the left crucible wall in the plane situated at 25 mm from the crucible bottom for $I = 2 \text{ A}$, 5 A and 10 A at $B = 3 \text{ mT}$, for a symmetrical electrodes positioning

In Figure VIII velocity profiles for the fluid flow at 5 mm from the crucible bottom are represented. All velocity profiles, regardless of the position, indicate higher positive velocity values in the area closer to the ultrasonic sensors. These remain positive along the profile which doesn't correspond to a rotation structure but are similar to those originating from a source. This (shown in schematically in Figure VIII) can originate from the flow in the vertical plane that was observed in the

planes situated at 25 mm and 40 mm. The melt, when it reaches the crucible bottom (from the secondary diagonal) is recirculated on the bottom going up in the opposite corner (or opposite walls).

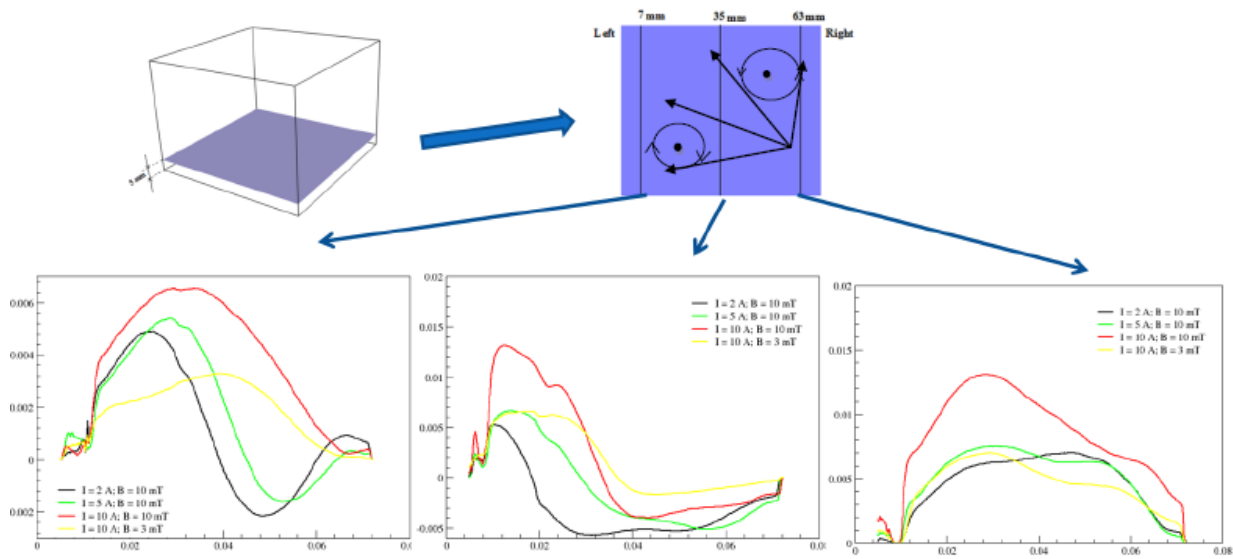


Figure VIII. Velocity profile along the axis of the three transducers placed at 9 mm, 35 mm and 61 mm from the left crucible wall in the plane situated at 5 mm from the crucible bottom for $I = 2$ A, 5 A and 10 A at $B = 3$ mT, for a symmetrical electrodes positioning

References:

- [1] Numerical study of different types of magnetic fields on the interface shape in directional solidification of multi-crystalline silicon ingots, C. Tanasie, D. Vizman, J. Friedrich, J. Crystal Growth, 318 (2011) 293-297

Project manager,